Vortex-lattice pinning in two-component Bose-Einstein condensates

M. P. Mink,[*] C. Morais Smith, and R. A. Duine

Institute for Theoretical Physics, Utrecht University, Leuvenlaan 4, 3584 CE Utrecht, The Netherlands

We investigate the vortex-lattice structure for single- and two-component Bose-Einstein condensates in the presence of an optical lattice, which acts as a pinning potential for the vortices. The problem is considered in the mean-field quantum Hall regime, which is reached when the rotation frequency Ω of the condensate in a radially symmetric trap approaches the (radial) trapping frequency ω and the interactions between the atoms are weak. We determine the vortex-lattice phase diagram as a function of optical-lattice strength and geometry. In the limit of strong pinning the vortices are always pinned at the maxima of the optical-lattice potential, similar to the slow-rotation case. At intermediate pinning strength, however, due to the competition between interactions and pinning energy, a structure arises for the two-component case where the vortices are pinned on lines of minimal potential.

I. INTRODUCTION

A characteristic property of a superfluid is that it supports angular momentum through quantized vortices [1,2]. If many vortices are present in the system, they arrange themselves in a hexagonal (Abrikosov) lattice [3]. The latter was observed experimentally in type-II superconductors [4,5] and more recently in a single-component Bose-Einstein condensate (BEC) [6,7]. In the case of rotating two-component condensates, the ground-state vortex lattice can have a nonhexagonal structure, since the vortices in both components can move with respect to each other. It was predicted that, among other structures, the vortex lattice in a two-component condensate can have an interlaced square structure [8]. This structure was indeed observed experimentally [9].

The Abrikosov lattice structure arises in a single-component BEC due to vortex-vortex interactions. One can also apply an optical-lattice potential to the condensate consisting of a regular pattern of potential minima and maxima. The prediction [10–12] that vortices are pinned at the maxima of an optical-lattice potential for sufficiently large strength was indeed confirmed experimentally [13]. Other theoretical work on rotating Bose gases in optical lattices focuses on the system near the superfluid–Mott-insulator transition [14–16] and on the effect of incommensurability between the vortex lattice and the optical lattice [17].

A remaining challenge is to determine the phase diagram of a rotating two-component condensate in an optical-lattice potential. Previous theoretical work focused on the slow-rotation limit and neglected the effect of the nonzero total particle density inside the vortex core [11]. In the interlaced vortex structure in a two-component BEC, the vortex lattices do not lie on top of each other, but are displaced by a fixed offset. This feature shows that the intercomponent interaction inside the vortex cores is important. Therefore, the approach from Ref. [11] is not suitable to determine all the vortex structures in rotating two-component BECs.

Here, we consider instead the mean-field quantum Hall regime, where the angular momentum of the condensate is so

high that the wave function resides in the lowest Landau level (LLL), but mean-field theory remains valid [18,19]. In this regime the wave function is completely determined by the positions of the vortices and no further approximations are needed. We extend the method from Refs. [8,18] to calculate the optical-lattice energy for a wave function in the LLL. The result is used to determine the phase diagram of a single-component condensate in an optical lattice of arbitrary geometry and a two-component condensate in a square optical lattice. For single-component condensates, we find phases in which the vortices are pinned on lines of maximal potential and phases in which they are pinned at the pinning centers, which is consistent with previous theoretical and experimental results [3,6,7,10–13]. In the two-component case, we find the interlaced square lattice in the absence of pinning and also a new phase where the vortices are pinned on lines of *minimal* potential.

The remainder of this paper is organized as follows. In Sec. II we evaluate the energy functional, including the optical lattice, of the system in the LLL regime. The result is used in Sec. III to determine the vortex phase diagrams of single- and two-component BECs in an optical lattice. In Sec. IV we present our conclusions.

II. VORTEX PINNING IN THE LLL: THEORY

We consider a rotating two-component BEC in an optical-lattice potential. In this section, we discuss the condensate wave function, the single-particle energies, and interaction energies in the LLL regime (see also Refs. [8,18]). Next, we evaluate the contribution of the optical-lattice potential to the energy of the system.

A. Energy functional

We are mainly interested in the two-dimensional (2D) ordering of the vortices. Therefore, we assume that the condensate has a small effective size d_z in the z direction and consider a 2D wave function. At the mean-field level, a two-component BEC is described by two macroscopic condensate wave functions $\psi_1(\mathbf{r})$ and $\psi_2(\mathbf{r})$, where $\mathbf{r}=(x,y)$.

*m.p.mink@uu.nl

The condensate rotates with an angular velocity Ω around the z axis; thus, it is convenient to transform to a frame that corotates with the condensate. The wave functions ψ_j describing the condensate are found by minimization of the energy functional in the rotating frame:

$$\mathcal{K} = \sum_{j=1,2} \left[\int d\mathbf{r} \psi_j^*(\mathbf{r})(h_j - \Omega L_z)\psi_j(\mathbf{r}) \right] + \mathcal{V}_I + \mathcal{V}_{OL}, \quad (1)$$

where ψ_j is normalized to the number of particles of species j, N_j. The single-particle Hamiltonians h_j are given by $h_j = -(\hbar^2/2M_j)\nabla^2 + M_j\omega^2 r^2/2$, with M_j the mass of a particle of species j, $\nabla = (\partial_x, \partial_y)$, $r = |\mathbf{r}|$, and ω is the frequency of the magnetic trapping potential in the radial direction, which we assume to be the same for particles of both species. The angular momentum operator is $L_z = -i\hbar\hat{\mathbf{z}}\cdot(\mathbf{r}\times\nabla)$. The interaction energy $\mathcal{V}_I$ in Eq. (1) reads

$$\mathcal{V}_I = \frac{1}{d_z} \int d\mathbf{r} \left(\frac{g_1}{2}|\psi_1(\mathbf{r})|^4 + \frac{g_2}{2}|\psi_2(\mathbf{r})|^4 + g_{12}|\psi_1(\mathbf{r})|^2|\psi_2(\mathbf{r})|^2 \right),$$
$$(2)$$

where the *intra-* and *intercomponent* interaction strengths are given by $g_j = 4\pi\hbar^2 a_j/M_j$ and $g_{12} = 2\pi\hbar^2 a_{12}/M_{12}$, respectively. Here, M_{12} is the reduced mass, and a_j and a_{12} denote the intra- and intercomponent scattering lengths, respectively. In this work we consider only repulsive interactions: $g_1, g_2, g_{12} > 0$. The optical-lattice potential couples to both species in the same way and its energy $\mathcal{V}_{OL}$ in Eq. (1) is given by

$$\mathcal{V}_{OL} = \int d\mathbf{r} V_{OL}(\mathbf{r})[|\psi_1(\mathbf{r})|^2 + |\psi_2(\mathbf{r})|^2], \quad (3)$$

where the optical-lattice potential is given by

$$V_{OL}(\mathbf{r}) = V_0[\cos(\mathbf{k}_1 \cdot \mathbf{r}) + \cos(\mathbf{k}_2 \cdot \mathbf{r})], \quad (4)$$

with the $\mathbf{k}_i$'s denoting the reciprocal optical-lattice vectors and V_0 the optical-lattice strength. The relation between the real-space optical-lattice vectors $\mathbf{b}_i$ and the $\mathbf{k}_i$'s is $\mathbf{k}_1 = (2\pi/A_{OL})\mathbf{b}_2 \times \hat{\mathbf{z}}$ and $\mathbf{k}_2 = -(2\pi/A_{OL})\mathbf{b}_1 \times \hat{\mathbf{z}}$, where $A_{OL} = |\mathbf{b}_1 \times \mathbf{b}_2|$ is the area of the unit cell of the optical lattice. We restrict our analysis to optical lattices which have a rhombus-shaped unit cell. The angle between the lattice vectors is denoted by ϕ.

B. Lowest Landau level

It is shown in Ref. [18] that in the absence of an optical lattice ($V_0 = 0$) and in the presence of a weak interaction ($\mathcal{V}_I$ small) the system enters the LLL regime when $\Omega \uparrow \omega$. This result can be easily extended to the case where $\mathcal{V}_{OL}$ is small. More specifically, the criterion is that interactions and the optical lattice do not cause transitions to higher-Landau-level states; i.e., it must hold that $g_j n_j, g_{12}\sqrt{n_1 n_2} \ll \hbar\omega$ and $V_0 \ll \hbar\omega$, where $\hbar\omega$ is the Landau-level gap and n_j is the density of species-j particles. In this regime, the macroscopic wave function ψ_j is completely determined by the position of the vortices and is given by

$$\psi_j(\mathbf{r}) = \lambda_j \prod_\alpha (z - \xi_\alpha^j)e^{-|z|^2/2\ell_j^2}, \quad (5)$$

where $\ell_j = \sqrt{\hbar/M_j\omega}$ is the magnetic length, $z = x + iy$ is the complex position coordinate, λ_j is a normalization constant, and $\{\xi_\alpha^j\}$ are the complex positions of the vortices in the condensate of species j.

We assume that the vortex positions in Eq. (5) form an infinite regular 2D lattice, and we project the functionals $\mathcal{V}_I$ and $\mathcal{V}_{OL}$ onto the space of wave functions with this property. The vortex lattice in condensate 1 is spanned by lattice vectors $\mathbf{c}_i$, which are parametrized as

$$\mathbf{c}_1 = \sqrt{\frac{A_{VL}}{p\sin\theta}}(1,0), \quad \text{and} \quad \mathbf{c}_2 = \sqrt{pA_{VL}\sin\theta}(\cot\theta, 1),$$

where $p = |\mathbf{c}_2|/|\mathbf{c}_1|$ is the ratio between the lengths, the angle between the $\mathbf{c}_i$'s is θ, and $\mathbf{c}_1$ lies along the x axis. Since, for a given lattice, the lattice vectors can always be chosen such that $p \geq 1$ and $\pi/3 \leq \theta \leq \pi/2$, we restrict p and θ to these ranges. The area of the vortex-lattice unit cell is $A_{VL} = |\mathbf{c}_1 \times \mathbf{c}_2|$. The reciprocal lattice vectors are $\mathbf{K}_1 = (2\pi/A_{VL})\mathbf{c}_2 \times \hat{\mathbf{z}}$ and $\mathbf{K}_2 = -(2\pi/A_{VL})\mathbf{c}_1 \times \hat{\mathbf{z}}$, where $\hat{\mathbf{z}}$ is the unit vector in the z direction. Note that within our approach it is not necessary that $A_{OL} = A_{VL}$. The vortex positions in the condensate 1 are given by $\Xi = \{m_i\mathbf{c}_i + \mathbf{v}_0\}$, where the m_i are integers, repeated indices $i \in \{1,2\}$ are summed over, and $\mathbf{v}_0$ is the offset of the vortex lattice in condensate 1 from the origin. Then, it holds for the particle density that

$$|\psi_1(\mathbf{r})|^2 = f(\mathbf{r} - \mathbf{v}_0)e^{-r^2/\sigma_1^2}, \quad \text{with} \quad \frac{1}{\sigma_1^2} = \frac{1}{\ell_1^2} - \frac{\pi}{A_{VL}},$$

where σ_1 is the effective condensate size in the radial direction and f is a structure function that is zero at the positions $\{m_i\mathbf{c}_i\}$ and has the lattice periodicity $f(\mathbf{r} + m_i\mathbf{c}_i) = f(\mathbf{r})$ [8,18]. In this paper, we want to study the situation in which the vortex lattices in both components are commensurate—i.e., in which they have the same geometry and unit-cell area. It is therefore natural to assume that atoms from species 1 and 2 are similar and to restrict our analysis to the case where $N_1 \simeq N_2$, $M_1 \simeq M_2$ and $g_1 \simeq g_2$. In the remainder, we drop the subscripts for these quantities. Thus, we assume that the vortex lattices in both components are the same, up to a constant offset $\mathbf{r}_0$: If the set of vortex positions in component 1 is Ξ, the set of vortex positions in component 2 is $\Xi + \mathbf{r}_0$. Then, both components are described by the same structure function f and have equal effective radial size $\sigma \equiv \sigma_1$ and equal vortex-lattice unit-cell area A_{VL}. Note that in contrast to the nonrotating case, the system will not phase separate when $g_{12} > \sqrt{g_1 g_2}$. The reason for this is that the system is already effectively phase separated (albeit incomplete), when it has an interlaced vortex-lattice structure [8]. The particle density in component 2 is given by

$$|\psi_2(\mathbf{r})|^2 = f(\mathbf{r} - \mathbf{v}_0 - \mathbf{r}_0)e^{-r^2/\sigma^2}.$$

When Ω is close to ω, the density spreads out in the radial direction, so that $\sigma^2/A_{VL} \gg 1$, and it can be shown [8] that the energy functional reads

$$\mathcal{K} = \frac{2N\hbar(\omega - \Omega)\sigma^2}{\ell^2} + \frac{gN^2}{2\pi\sigma^2 d_z}(I + \widetilde{g}_{12}I_{12}) + \mathcal{V}_{\text{OL}}, \quad (6)$$

where $\widetilde{g}_{12} = g_{12}/g$. The first term in Eq. (6) is the contribution from the single-particle Hamiltonians h_j. The quantities I and I_{12} describe the intra- and intercomponent interaction energy, respectively, and are given by

$$I = \sum_{\mathbf{K}} |f_{\mathbf{K}}|^2, \quad \text{and} \quad I_{12} = \sum_{\mathbf{K}} |f_{\mathbf{K}}|^2 \cos(\mathbf{K} \cdot \mathbf{r}_0), \quad (7)$$

where the $f_{\mathbf{K}}$ are the Fourier coefficients of the function $f(\mathbf{r})$ and are given by

$$f_{\mathbf{K}} = (-1)^{m_1 + m_2 + m_1 m_2} e^{-A_{\text{VL}}\mathbf{K}^2/8\pi} \quad (8)$$

for a reciprocal lattice vector $\mathbf{K} = m_1\mathbf{K}_1 + m_2\mathbf{K}_2$, with m_1 and m_2 integers. In the next section we calculate $\mathcal{V}_{\text{OL}}$.

C. Optical-lattice energy

Using the Fourier expansion of the function $f(\mathbf{r})$, we normalize the particle densities $|\psi_j(\mathbf{r})|^2$ to N:

$$|\psi_1(\mathbf{r})|^2 = \frac{N}{\pi\sigma^2}\sum_{\mathbf{K}} \widetilde{f}_{\mathbf{K}} e^{i\mathbf{K}\cdot(\mathbf{r}-\mathbf{v}_0)} e^{-r^2/\sigma^2},$$

$$|\psi_2(\mathbf{r})|^2 = \frac{N}{\pi\sigma^2}\sum_{\mathbf{K}} \hat{f}_{\mathbf{K}} e^{i\mathbf{K}\cdot(\mathbf{r}-\mathbf{v}_0-\mathbf{r}_0)} e^{-r^2/\sigma^2},$$

where we defined $\widetilde{f}_{\mathbf{K}} = f_{\mathbf{K}}/\sum_{\mathbf{K}'} f_{\mathbf{K}'} e^{-i\mathbf{K}'\cdot\mathbf{v}_0} e^{-\sigma^2\mathbf{K}'^2/4}$ and $\hat{f}_{\mathbf{K}} = f_{\mathbf{K}}/\sum_{\mathbf{K}'} f_{\mathbf{K}'} e^{-i\mathbf{K}'\cdot(\mathbf{r}_0+\mathbf{v}_0)} e^{-\sigma^2\mathbf{K}'^2/4}$. We use the fact that when $\Omega \to \omega$, it holds that $\sigma^2/A_{\text{VL}} \gg 1$, and since $\mathbf{K}^2 \sim 1/A_{\text{VL}}$ if $\mathbf{K} \neq 0$, only those terms in the summations in the denominators of $\widetilde{f}_{\mathbf{K}}$ and $\hat{f}_{\mathbf{K}}$ for which $\mathbf{K} = 0$ survive. Hence, $\widetilde{f}_{\mathbf{K}} = \hat{f}_{\mathbf{K}} = f_{\mathbf{K}}$. By substituting the expressions for $|\psi_1(\mathbf{r})|^2$ and $|\psi_2(\mathbf{r})|^2$ into Eq. (3) we find

$$\mathcal{V}_{\text{OL}} = \frac{NV_0}{2}\sum_{\mathbf{K},j} f_{\mathbf{K}} e^{-i\mathbf{K}\cdot\mathbf{v}_0}(1 + e^{-i\mathbf{K}\cdot\mathbf{r}_0})G_{j,\mathbf{K}},$$

where

$$G_{j,\mathbf{K}} = \frac{2}{\pi\sigma^2}\int d\mathbf{r} e^{i\mathbf{K}\cdot\mathbf{r}} e^{-r^2/\sigma^2}\cos(\mathbf{k}_j \cdot \mathbf{r})$$

$$= (e^{-(\mathbf{K}+\mathbf{k}_j)^2\sigma^2/4} + e^{-(\mathbf{K}-\mathbf{k}_j)^2\sigma^2/4}).$$

We again use the fact that in the fast-rotating limit $(\mathbf{K}+\mathbf{k}_j)^2\sigma^2 \gg 1$ or $(\mathbf{K}-\mathbf{k}_j)^2\sigma^2 \gg 1$ unless $\mathbf{K} = -\mathbf{k}_j$ or $\mathbf{K} = \mathbf{k}_j$, respectively. Thus, the Gaussian terms of $G_{j,\mathbf{K}}$ are very small unless their argument is zero. Therefore, it is reasonable to approximate $G_{j,\mathbf{K}}$ by the sum of two Kronecker delta's: $G_{j,\mathbf{K}} = \delta_{\mathbf{K},\mathbf{k}_j} + \delta_{-\mathbf{K},\mathbf{k}_j}$. Using that $G_{j,\mathbf{K}}$ and $f_{\mathbf{K}}$ are even in $\mathbf{K}$, we find that

$$\mathcal{V}_{\text{OL}} = NV_0\sum_{\mathbf{K},j} f_{\mathbf{k}_j}\delta_{\mathbf{K},\mathbf{k}_j}\{\cos(\mathbf{k}_j \cdot \mathbf{v}_0) + \cos[\mathbf{k}_j \cdot (\mathbf{v}_0 + \mathbf{r}_0)]\}.$$

$$(9)$$

From Eq. (9) it follows that the system can only gain pinning energy if there are reciprocal vortex-lattice vectors

$\mathbf{K}$ equal to $\mathbf{k}_1$ and/or $\mathbf{k}_2$. In that case the vortices are pinned on equally spaced lines, as we show below. Assume for concreteness that $\mathbf{k}_1 = \mathbf{K} = m_1\mathbf{K}_1 + m_2\mathbf{K}_2$, with m_1 and m_2 integers. Using the definitions of the reciprocal optical-lattice and vortex-lattice vectors given above, this is equivalent to $m_1\mathbf{c}_1 - m_2\mathbf{c}_2 = (A_{\text{VL}}/A_{\text{OL}})\mathbf{b}_2$. Since the $\mathbf{c}_i$'s are linearly independent vectors, there is a pair of *real* numbers (r_1, r_2) such that $r_1\mathbf{c}_1 + r_2\mathbf{c}_2 = \mathbf{b}_1$. By taking outer products between the left- and right-hand sides of the last two equalities, we obtain $|m_1r_2 + m_2r_1| = 1$. By inverting the expressions for the $\mathbf{b}_i$'s, we reach the conclusion that the coefficient of $\mathbf{b}_1$ in the expansion of both $\mathbf{c}_i$'s is an integer. Thus, the vortices are pinned on the collection of lines $\{n\mathbf{b}_1 + r\mathbf{b}_2 + \mathbf{v}_0, n \in \mathbb{Z} \text{ and } r \in \mathbb{R}\}$. Analogously, we can show that if there is a reciprocal vortex-lattice vector $\mathbf{K}$ equal to $\mathbf{k}_2$, the vortices are pinned on the lines $\{r\mathbf{b}_1 + n\mathbf{b}_2 + \mathbf{v}_0, n \in \mathbb{Z} \text{ and } r \in \mathbb{R}\}$. Since vortices are density minima, one intuitively expects that the lines are always lines of maximal potential and that $\mathbf{v}_0 = 0$. Nonetheless, it turns out that in the two-component case there are regions in the phase diagram that have nonzero $\mathbf{v}_0$.

In the case that there are reciprocal vortex-lattice vectors $\mathbf{K}_a$ and $\mathbf{K}_b$, equal to $\mathbf{k}_1$ and $\mathbf{k}_2$, respectively, the vortex positions lie at the intersection of the two collections of lines we mentioned above—i.e., on the positions $\{m_1\mathbf{b}_1 + m_2\mathbf{b}_2 + \mathbf{v}_0, m_i \in \mathbb{Z}\}$.

III. VORTEX PINNING IN THE LLL: PHASE DIAGRAMS

In this section we determine phase diagrams of single- and two-component BECs using the results for the energy functional in Eqs. (6)–(8) and the optical-lattice energy, Eq. (9). We consider first the case of a single-component condensate in an optical lattice with arbitrary unit-cell angle and then the case of a two-component condensate in a square optical lattice. For simplicity, we restrict our analysis to vortex lattices with one vortex per optical-lattice unit cell—i.e., to the case $A_{\text{VL}} = A_{\text{OL}} \equiv A$. Then, the first term in Eq. (6) is a constant, which we drop.

A. Single-component lattices

For the single-component case, the energy $\mathcal{K}_s$ of a condensate of N particles in an optical lattice is found from Eq. (6) by setting $\widetilde{g}_{12}$ and $\mathbf{r}_0$ to zero and dividing all terms by a factor of 2:

$$\mathcal{K}_s = \frac{gN^2}{4\pi\sigma^2 d_z}I + NV_0\sum_{\mathbf{K},j} f_{\mathbf{k}_j}\delta_{\mathbf{K},\mathbf{k}_j}\cos(\mathbf{k}_j \cdot \mathbf{v}_0).$$

In Fig. 1 we display the phase diagram, which is obtained by numerical minimization of $\mathcal{K}_s$ as a function of the vortex-lattice parameters for given optical-lattice angle ϕ and strength V_0. The latter is represented in units of $\mu_0 \equiv gN/\pi\sigma^2 d_z$, which is equal to the chemical potential μ, up to a numerical factor of order 1. The unpinned, line-pinned, and fully pinned phases are indicated by UP, LP, and FP, respectively. We describe these phases below.

In the *unpinned phase*, there is no $\mathbf{K}$ equal to $\mathbf{k}_1$ or $\mathbf{k}_2$ and the last term of $\mathcal{K}_s$ is zero. The vortex lattice ignores the optical lattice, and the relative orientation of the two lattices
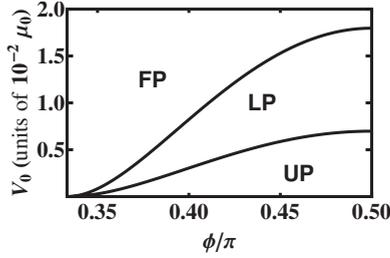
FIG. 1. Phase diagram for a single-component BEC in an arbitrary optical-lattice potential. On the horizontal axis, we show the angle ϕ of the optical lattice, from $\phi=\pi/3$ (hexagonal lattice) to $\phi=\pi/2$ (square lattice). On the vertical axis, we show the optical-lattice strength V_0 in units of $\mu_0 \equiv gN/\pi\sigma^2 d_z$. The unpinned, line-pinned, and fully pinned phases are indicated by UP, LP, and FP, respectively. All lines denote first-order phase transitions.

is not correlated. The incommensurability between the vortex- and optical-lattice causes the optical-lattice potential energy to average to zero. The optimal unpinned vortex lattice has $p=1$ and $\theta=\pi/3$. This corresponds to the Abrikosov structure, and the result is consistent with experimental and theoretical results obtained outside the LLL regime [6,7].

The *line-pinned phase* for an arbitrary optical-lattice angle ϕ is shown in Fig. 2(a), where the x axis is in the direction of the dashed lines. In this phase the vortices (circles) are pinned on the (dashed) lines of maximal potential, specified by $\{r\mathbf{b}_1+n\mathbf{b}_2, n \in \mathbb{Z} \text{ and } r \in \mathbb{R}\}$. The pinning centers are not shown, but they are located on the dashed lines. It holds that $\mathbf{c}_1=\mathbf{b}_1$, $\mathbf{v}_0 \cdot \hat{\mathbf{y}}=0$, and the lattice vector $\mathbf{c}_2$ is such that the line-pinned vortex lattice resembles the Abrikosov lattice structure the closest: $\mathbf{c}_2=\mathbf{b}_1/2+(\mathbf{b}_2 \cdot \hat{\mathbf{y}})\hat{\mathbf{y}}$. The energy does not depend on the x coordinate of $\mathbf{v}_0$: if we shift the vortex lattice in the horizontal direction, its energy does not change. For the optical-lattice angle $\phi=\pi/3$, the line-pinned vortex lattice has precisely the Abrikosov lattice structure.

The *fully pinned phase* is shown in Fig. 2(b) for the square optical lattice. Here, all vortices are pinned on the maxima of the optical lattice, which are represented by crosses: $\mathbf{c}_1=\mathbf{b}_1$, $\mathbf{c}_2=\mathbf{b}_2$, and $\mathbf{v}_0=0$. The vortex lattice exactly matches the geometry of the optical lattice.

If we start in Fig. 1 in the unpinned phase in the case of a square optical lattice ($\phi=\pi/2$) and increase the strength V_0,
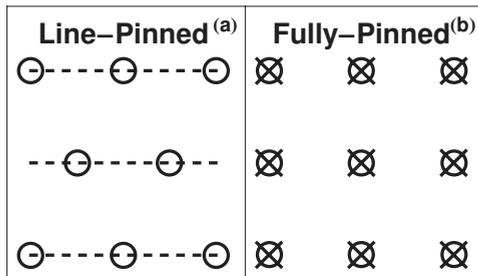

FIG. 2. The line-pinned and fully pinned vortex lattices for the case of an arbitrary optical-lattice angle ϕ and a square optical lattice, respectively. The dashed lines are lines of maximal potential; the vortices are represented by circles. In (a) the pinning centers (not shown) are located on the dashed lines, and in (b) they are represented by the crosses.
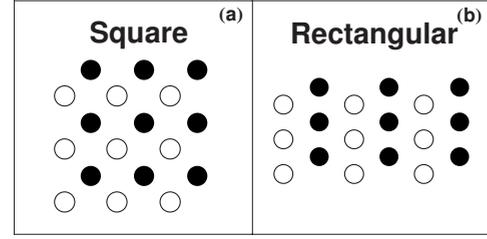

FIG. 3. The interlaced square and rectangular vortex lattices in a two-component condensate in the absence of pinning. The open (solid) circles correspond to vortices in component 1 (2). For further details we refer the reader to Ref. [8].

there is a first-order transition to the line-pinned phase at $V_0=0.007\mu_0$. When we increase V_0 even further, we find another first-order transition from the line-pinned to the fully pinned phase at $V_0=0.018\mu_0$. The transitions are caused by the fact that the system can gain pinning energy by transforming to a state in which the vortices are pinned on the lines or points of maximal potential. For optical-lattice angles $\phi<\pi/2$, one observes that a smaller optical-lattice strength V_0 is sufficient to trigger the transitions from the unpinned to the line-pinned and from the line-pinned to the fully pinned phase. At optical-lattice angle $\phi=\pi/3$, it takes an infinitesimal V_0 to achieve orientation locking. These observations can be explained by the fact that for lower optical-lattice angles ϕ the fully pinned and line-pinned structures resemble more closely the hexagonal Abrikosov lattice structure, which is the optimal structure in the absence of pinning.

The orientation locking of the vortex lattice in a hexagonal optical lattice ($\phi=\pi/3$) was observed experimentally [13]. Contrary to our results, the authors found that a nonzero minimum pinning strength is needed for orientation locking, which they suggest is due to long equilibration times of the system. Such nonequilibrium effects cannot be investigated with the equilibrium theory presented here. The fully pinned phase for a square optical lattice ($\phi=\pi/2$) was also found earlier [10,12,13]. The structural lattice transitions in Fig. 1 typically occur for $V_0 \approx 0.01\mu_0 \approx 0.01\mu$, which is in rough agreement with previous theoretical predictions [10,12] and experimental observations [13]. Note that our line-pinned phase is similar to the pinned phase found in Ref. [10] for a *one-dimensional* optical lattice, although the geometry of the optical lattice in our system is *two dimensional*. Furthermore, we note that the half-pinned phase mentioned in Refs. [10,11] is equivalent to the line-pinned phase for $\phi=\pi/2$.

B. Two-component lattices

The energy functional $\mathcal{K}$ of a rotating two-component condensate in an optical lattice is given by Eqs. (6)–(9). In Ref. [8], the system was analyzed in the absence of pinning, where $V_0=0$. The authors found that the structure of the ground-state vortex lattice depends on the value of $\tilde{g}_{12}$. We show two possible configurations for $V_0=0$ in Fig. 3, where the open (solid) circles correspond to vortices in component 1 (2). The interlaced square structure, mentioned in the Introduction, is the ground state when $0.37<\tilde{g}_{12}<0.93$ [see
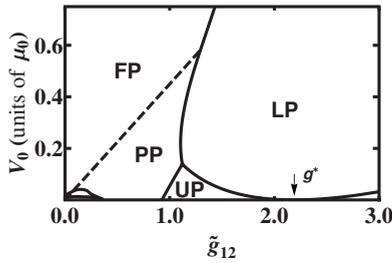
FIG. 4. Vortex phase diagram of a two-component condensate in the presence of a square optical lattice. On the horizontal axis, we show the scaled intercomponent interaction strength $\tilde{g}_{12}$ and on the vertical axis the optical-lattice strength V_0 in units of μ_0. Solid (dashed) lines denote first-order (second-order) phase transitions.

Fig. 3(a)]. For $\tilde{g}_{12} > 0.93$, the vortex lattice deforms into a rectangular structure, as shown in Fig. 3(b). The ratio between the lengths of the two vortex-lattice vectors p continuously increases with increasing $\tilde{g}_{12}$. For further details we refer the reader to Ref. [8].

The vortex phase diagram of a two-component condensate in the presence of a *square* optical lattice is shown in Fig. 4. On the horizontal axis we show the scaled intercomponent interaction strength $\tilde{g}_{12}$ and on the vertical axis the optical-lattice strength V_0 in units of μ_0. In the figure, solid lines denote first-order and dashed lines second-order phase transitions. The left below corner of the phase diagram contains unpinned phases which are described in Ref. [8] and a line-pinned phase which is a trivial extension to the two-component case of the single-component line-pinned phase shown in Fig. 2(a). We will not discuss these phases further. At larger values of $\tilde{g}_{12}$ and/or V_0, novel phases arise. In the pair-pinned (PP) structure [see Fig. 5(a)], the vortex lattice consists of pairs of a component-1 and a component-2 vortex, which form a square lattice. The vortices in a pair are displaced by $\mathbf{r}_0 = r(\mathbf{c}_1 + \mathbf{c}_2)$ with respect to each other, and the pairs are pinned at the optical-lattice maxima in such a way that the vortices in a pair lie at equidistant positions from their pinning center. In Fig. 5(a), we encircled one of these vortex pairs for clarity. The value of r at $V_0 = 0$ is 0.5, so that the vortex lattice has the interlaced square structure shown in Fig. 3(a). When we increase V_0, the value of r decreases

continuously from 0.5 to 0. The system gains pinning energy if the vortices in a pair move closer together towards the pinning center. When $r = 0$, the system enters the fully pinned phase through a second-order phase transition. In this phase, the vortices in a pair are pinned on top of each other at the potential maxima, analogous to the fully pinned single-component vortex lattice in Fig. 2(b).

At low values of V_0 and for $\tilde{g}_{12} \approx 1.2$ and $\tilde{g}_{12} \approx 3$, the system is in the unpinned interlaced rectangular structure [see Fig. 3(b)], which we denote by UP. At the value $\tilde{g}_{12} = 2.19 \equiv g^*$, the ratio p between lengths of the lattice vectors of the unpinned rectangular lattice is equal to 4. Then, the rectangular vortex lattice is commensurate with the square optical lattice and can be line pinned by an arbitrarily weak optical lattice. For values of $\tilde{g}_{12}$ close to (but unequal to) g^*, the transition to the line-pinned phase is first order and occurs at small, but finite values of V_0. In terms of lattice vectors, this phase is specified by $\mathbf{c}_1 = \mathbf{b}_1/2$, $\mathbf{c}_2 = 2\mathbf{b}_2$, and $\mathbf{r}_0 = (\mathbf{c}_1 + \mathbf{c}_2)/2$. Interestingly, the lines on which the vortices in this phase are pinned are not the lines of maximal potential, as one would expect intuitively, but the lines of minimal potential, which is opposite to the single-component case in Fig. 2(a). The reason is that the *total* density is not minimal on the (horizontal) lines on which the vortices lie, but halfway between those lines. It follows from Eq. (5) that the healing length of vortices in the LLL regime is equal to the distance between the vortices and this causes the above-mentioned location of the minima in the total density. The minima in the *total* density *are* pinned on lines of maximal potential, as expected.

IV. DISCUSSION AND CONCLUSIONS

In summary, we have considered vortex lattices in single- and two-component BECs in a 2D optical-lattice potential in the LLL regime. We have incorporated the effects due to the optical lattice and determined the phase diagram of a single-component condensate in an optical-lattice potential with arbitrary unit-cell angle and of a two-component condensate in a square optical-lattice potential. For the single-component case, we find, among others, phases that are pinned on lines of maximal potential or at the potential maxima. In the two-component case, we find a phase in which pairs of vortices are pinned at the potential maxima and a phase where vortices are pinned on the lines of *minimal* potential. Note that Ref. [16] also points out the possibility of pinning at the minima of the optical-lattice potential, albeit in a different regime than we consider here.

As mentioned before, the criteria for the validity of the LLL assumption are that the interaction energy per particle gn and the optical-lattice strength V_0 be much smaller than the LLL gap $\hbar\omega$. Full pinning typically occurs at $V_0 = 0.01\mu_0$ ($V_0 = 0.1\mu_0$) for single-component (two-component) condensates, so that at these typical values ($V_0 \ll \mu_0 \approx gn$) the LLL condition remains valid. This difference in optical-lattice strength comes about because of the difference in vortex filling factors considered. We do not expect fundamental obstacles for observing vortex pinning in a two-component condensate, since the rotation velocities for which vortex
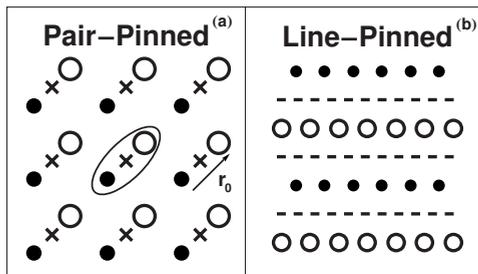

FIG. 5. The pair-pinned and line-pinned two-component vortex lattices. The crosses indicate the location of the pinning centers, the open circles the vortices of in component 1, and the solid circles those in component 2. The horizontal dashed lines are lines of maximal potential. In (b) the pinning centers (not shown) are located on the dashed lines.

pinning in a single-component BEC and the interlaced square lattice structure in a two-component BEC without pinning were observed are similar [9,13]. Our results are consistent with theoretical [10,11] and experimental [13] work for single-component condensates in an optical lattice and two-component condensates without pinning [9], which were performed *outside* the LLL regime. Hence, we expect that our results are, at least qualitatively, valid also outside the LLL regime.

A possibility for further research is to relax the restriction that there be one or two vortices per optical-lattice unit cell and study the effect of incommensurability between the vor-

tex lattice and the optical lattice. In particular, it is interesting to investigate the situation in which the unit cell of the optical lattice is smaller than the critical vortex-lattice unit-cell size $\pi\ell^2$, which would require an extension of the formalism presented here.

[1] L. Onsager, Nuovo Cimento, Suppl. **6**, 249 (1949).

[2] R. P. Feynman, in *Progress in Low Temperature Physics*, edited by C. J. Gorter (North-Holland, Amsterdam, 1955), Vol. 1, p. 17.

[3] A. A. Abrikosov, Zh. Eksp. Teor. Fiz. **32**, 1142 (1957) [Sov. Phys. JETP **5**, 1174 (1957)].

[4] S. J. Tsakadze, Fiz. Nizk. Temp. **4**, 148 (1978) [Sov. J. Low Temp. Phys. **4**, 72 (1978)].

[5] E. J. Yarmchuk, M. J. V. Gordon, and R. E. Packard, Phys. Rev. Lett. **43**, 214 (1979).

[6] K. W. Madison, F. Chevy, W. Wohlleben, and J. Dalibard, Phys. Rev. Lett. **84**, 806 (2000).

[7] J. R. Abo-Shaeer, C. Raman, J. M. Vogels, and W. Ketterle, Science **292**, 476 (2001).

[8] Erich J. Mueller and Tin-Lun Ho, Phys. Rev. Lett. **88**, 180403 (2002).

[9] V. Schweikhard, I. Coddington, P. Engels, S. Tung, and E. A. Cornell, Phys. Rev. Lett. **93**, 210403 (2004).

[10] J. W. Reijnders and R. A. Duine, Phys. Rev. Lett. **93**, 060401 (2004).

[11] J. W. Reijnders and R. A. Duine, Phys. Rev. A **71**, 063607 (2005).

[12] H. Pu, L. O. Baksmaty, S. Yi, and N. P. Bigelow, Phys. Rev. Lett. **94**, 190401 (2005).

[13] S. Tung, V. Schweikhard, and E. A. Cornell, Phys. Rev. Lett. **97**, 240402 (2006).

[14] Congjun Wu, Han-dong Chen, Jiang-piang Hu, and Shou-Cheng Zhang, Phys. Rev. A **69**, 043609 (2004).

[15] E. Lundh, Europhys. Lett. **84**, 10007 (2008).

[16] Daniel S. Goldbaum and Erich J. Mueller, Phys. Rev. A **77**, 033629 (2008).

[17] Daniel S. Goldbaum and Erich J. Mueller, e-print arXiv:0809.2078v1.

[18] Tin-Lun Ho, Phys. Rev. Lett. **87**, 060403 (2001).

[19] N. R. Cooper, e-print arXiv:0810.4398v1.